Imidazole derivatives as promising agents for the treatment of Chagas disease[†]

RUNNING TITLE: Imidazoles: antichagasic agents

Julianna Siciliano de Araújo,[a,§] Alfonso Garcia-Rubia,[b,§] Victor Sebastian-Perez,[b,§] Titilola D. Kalejaiye,[c] Patrícia Bernardino da Silva,[a] Cristina Rosa Fonseca-Berzal,[a,d] Louis Maes,[e] Harry P. De Koning,[c] Maria de Nazaré Correia Soeiro[a,*] and Carmen Gil[b,*]

[a]Laboratório de Biologia Celular, Instituto Oswaldo Cruz, Fundação Oswaldo Cruz, Rio de Janeiro, Brazil

[b]Centro de Investigaciones Biológicas (CSIC). Ramiro de Maeztu, 9, 28040 Madrid, Spain

[c]Institute of Infection, Immunity and Inflammation, University of Glasgow, United Kingdom

[d]Departamento de Parasitología, Facultad de Farmacia, Universidad Complutense de Madrid, Madrid, Spain

[e]Laboratory for Microbiology, Parasitology and Hygiene (LMPH), University of Antwerp, Belgium

[†] This paper is dedicated to the memory of our friend and colleague, Prof. Mercedes González

[§] These authors have contributed equally to this work

* Corresponding author

ABSTRACT. More than 100 years later after being firstly described, Chagas disease remains endemic in 21 Latin American countries and has spread to other continents. Indeed, this disease, caused by the protozoan parasite *Trypanosoma cruzi*, is no longer just a problem for the American continent but has become a global health threat. Current therapies, nifurtimox and benznidazole (Bz), are far from being adequate due to undesirable effects and their lack of efficacy in the chronic phases of the disease. In this work, we present an in-depth phenotypical evaluation in *T.cruzi* of a new class of imidazole compounds, discovered in a previous phenotypic screening against different trypanosomatids and designed as potential inhibitors of cAMP phosphodiesterases (PDEs). The confirmation of several activities similar or superior to Bz prompted a synthesis program of hit optimization and extended SAR, aimed at improving drug-like properties such as aqueous solubility, resulting in additional hits with IC_{50} similar to Bz. The cellular effects of one representative hit compound **9** (NPD-274), on bloodstream trypomastigotes were further investigated. Transmission electron microscopy revealed cellular changes, after just 2 h of incubation with the IC_{50} concentration, that were consistent with induced autophagy and osmotic stress - mechanisms previously linked to cAMP signaling. **9** (NPD-274) induced highly significant increases in both cellular and medium cAMP, confirming that inhibition of (a) *T.cruzi* PDE(s) is part of its mechanism of action. The potent and selective activity of this imidazole-based PDE inhibitor class against *T.cruzi* constitutes a successful repurposing of research into inhibitors of mammalian PDEs.

KEYWORDS: Drug Discovery, Chagas Disease, imidazole

INTRODUCTION

Parasites belonging to the order Kinetoplastida are responsible for public health concerns worldwide and cause extensive human suffering and death. Among these protozoan flagellates are *Trypanosoma brucei* spp (*T. b. gambiense* and *T. b. rhodesiense*) and *T. cruzi* (agents of human African trypanosomiasis and American trypanosomiasis, respectively), besides various *Leishmania* spp, which cause leishmaniasis (1).

American trypanosomiasis, also known as Chagas disease (CD), was described in 1909 by the Brazilian researcher Carlos Chagas (2). More than 100 years later, this neglected tropical disease remains endemic in 21 countries from Latin America according to the WHO (3). Moreover, although the disease was confined to the Region of the Americas, over the last century, it has spread to other continents mainly due to human migration (4).

CD is mainly transmitted by blood-sucking reduviid insects in endemic countries, but other infection routes include vertical transmission, orally via contaminated beverages and food, blood transfusion and organ transplantation, among others (2). The disease has an acute phase that occurs immediately after the infection and is usually asymptomatic/oligosymptomatic. The extent of parasite proliferation is controlled by a competent host immune response, although the patient remains chronically infected if untreated. Many of them could remain asymptomatic, but 30-40% develop a severe stage that is mainly characterized by cardiac and/or gastrointestinal pathologies (5). Chemotherapy is highly recommended for all acute and chronic asymptomatic infected patients, but the current drugs, nifurtimox and benznidazole, are far from adequate due to side effects and their poor efficacy in all clinical phases (especially inactive against the chronic phase), besides the occurrence of naturally resistant parasite strains belonging to some different discrete typing units (DTUs) (6).

For these reasons, the search for effective, well-tolerated and affordable CD drugs is both urgent and of genuine importance. However, despite significant advances in the discovery and development of new effective drugs for this tropical disease, it remains an unmet clinical need (7, 8) and for many patients there is no effective treatment. This paper describes the therapeutic potential of a class of imidazole compounds discovered to have anti-protozoan activity in a previous phenotypic screening against different trypanosomatids of different human PDE inhibitors from our in-house chemical library (9). Compounds from this chemical class showed potential utility in Parkinson's disease due to its ability to inhibit mammalian cyclic nucleotide PDE10A (10). The work includes an evaluation of the mechanism of action of this compound class, and initial efforts towards hit optimization and the development of a structure-activity relationship (SAR).

RESULTS

Optimization of imidazole hit compounds. A previous phenotypic screen of a focused library of 69 imidazole derivatives in a panel of three pathogenic trypanosomatids, *T. brucei*, *T. cruzi* and *L. infantum,* highlighted these imidazoles as promising hits for the development of anti-*Leishmania* therapy (9). Interestingly, twelve members of this library (compounds **1**-**12**) showed also promising activities against the intracellular forms of *T. cruzi* (Tulahuen-β-galactosidase-transfected parasites, DTU VI), some of them being in a quite similar potency as benznidazole (Bz; IC_{50} = 3.18 μM) (Table S1 from the Supplemental Material), justifying further analysis of their potential against *T. cruzi*, including chemical optimization.

The first priority was to improve the drug-like properties of the compounds with the most interesting anti-*T. cruzi* imidazoles. In order to improve aqueous solubility, we decided to increase the polarity, designing a new serie of imidazole-related compounds

with a reduced number of aromatic rings as substituents on the heterocyclic core and introducing a polar group such as the urea moiety.

The first synthetic approach to obtain these newly designed compounds used different aminothiazole and aminoimidazole derivatives as starting material, together with different isocyanates to easily synthesize the corresponding urea in one step, by microwave irradiation in tetrahydrofuran (THF) with low to moderate yields (Scheme 1). The second approach was focused on a 4-phenyl-2-amino imidazole scaffold and employed a two-step synthesis based on the use of 1,1'-carbonyldiimidazole (CDI) as reagent to convert the amino group into urea. After addition of CDI to the aminoimidazole, the amine is activated and a carbonyl group added. The addition of the corresponding substituted amine then allowed the formation of the final urea derivative with moderate yields (Scheme 2).

Thus, 26 new imidazole-related compounds bearing a urea motif were synthesized and evaluated against the standard panel (9) of *T. brucei*, *T. cruzi* and *L. infantum*, and their cytotoxicity evaluated on human lung fibroblast (MRC-5) and primary cultures of peritoneal mouse macrophages (PMM) (Table 1). Among the new synthesized compounds, thiazole derivatives (**13**-**17**) were not active at all, while the most promising compounds (**23** (NPD-3032), **31** (NPD-3126), **33** (NPD-3024), **37** (NPD-3124) and **38** (NPD-3125)) against intracellular β-galactosidase-transfected *T. cruzi* (Tulahuen- strain, DTU VI) were imidazole derivatives bearing a urea motif in position 2. Remarkably, fluoride substituents look like to be favorable for the activity against *T. cruzi* (trifluoromethyl at position 4 of R^2 substituent in **33**, **37** and **38**; trifluoromethoxy at position 4 of one of the phenyl substituents in **23**). Moreover, the activity of most of these compounds was specific to *T. cruzi*, although some activity was observed against the other trypanosomatids as well, particularly against the closely related *T. brucei*; crucially they displayed little or no toxicity to the mammalian cell lines. The fact that the introduction of the polar urea group was well tolerated and in some cases actually

enhanced the selective anti-*T. cruzi* activity is very encouraging for further exploration in this chemical space.

[Here, Schemes 1 and 2]

[Here, Table 1]

Activity against bloodstream trypomastigotes. In order to verify the therapeutic potential of this new compound class, we phenotypically assayed the original imidazole hits (**1**-**12**) (Table S1) and the most promising of the new 4-phenyl, 2-ureaimidazoles **23**, **31**, **33**, **37** and **38** (*i.e.* all the derivatives with an IC_{50} below 10 μM) against the other parasite form relevant for the mammalian infection (bloodstream trypomastigotes – BT). To address the possibility that the compounds might not be effective against other *T. cruzi* DTUs, we assayed also another strain from a different DTU (Y strain - DTU II) for this assay. We found that 5 of the 17 compounds tested showed greater activity than Bz (IC_{50} = 12.9 ± 1.9 μM) against Y strain BT, with IC_{50} values ranging 1.2 - 11.5 μM (Table 2). Compound **9** (NPD-274) stood out as the most active against this life-cycle stage (IC_{50} = 1.2 ± 0.3 μM). As heart muscle is an important target for *T. cruzi* infection and inflammation, we also investigated the potential toxicity of these compounds towards primary cultures of mouse cardiac cells. As shown in Table 2, most compounds were not cardiotoxic, exhibiting LC_{50} values ranging from 65 up to > 200 μM. The selective index was calculated, showing **9** (NPD-274) to be the most selective (SI > 85) followed by **33** (NPD-3024) (IC_{50} = 4.6 ± 0.1 μM, SI > 44).

[Here, Table 2]

Cellular effects of 9 (NPD-274). Imidazole **9** (NPD-274) was chosen for further analysis of the cellular effects of the imidazole compound class. Bloodstream

157 trypomastigotes of Y strain were incubated for 2 h with 1×EC_{50} of **9** (NPD-274) and the
158 effects on their ultrastructure were analysed using transmission electron microscopy
159 (Figure 1). Treated parasites exhibited severe features that included flagellar pocket
160 dilatation, disruption of Golgi apparatus, extensive blebs and shedding events of the
161 plasma membrane, in addition to a large number of myelin figures and membranous
162 profiles surrounding cytoplasmic organelles - an apparent sign of autophagy.
163
164 [Here, Figure 1]
165
166 As related imidazoles were found to be able to increase cAMP levels in *Leishmania*
167 promastigote cultures (9), we here tested whether **9** (NPD-274) was similarly able to
168 increase the levels of this cyclic nucleotide in *T. cruzi*. With this aim, BT of Y strain
169 were incubated with either 2× or 5×EC_{50} of this compound for 2.5 h, and both the
170 cellular cAMP content and the released cAMP in the medium determined. Cultures
171 incubated in parallel, either without test compound, or with known *T. brucei* PDE
172 inhibitors (NPD-001 (11) and NPD-008 (12)), served as negative and positive controls,
173 respectively.
174 Our data demonstrated that incubation with **9** (NPD-274) dose-dependently increased
175 the intracellular content of cAMP (1.8-fold, P <0.05, and 2.5-fold of untreated control, P
176 <0.01, at 2× and 5×EC_{50}, respectively) (Figure 2A). cAMP was also released from the
177 cells and could be measured in the medium; NPD-001, NPD-008 and **9** (NPD-274) all
178 induced highly significant increases in the extracellular cAMP concentration relative to
179 the untreated control (P <0.001; Figure 2B).
180
181 [Here, Figure 2]
182
183 **DISCUSSION**

184 Today, Chagas disease is no longer only a problem for Latin America but has become
185 a global public health threat. Current therapeutic options rely on only two (related:
186 nitrofuran or nitroimidazole) drugs, nifurtimox and benznidazole, that although active in
187 the acute phase of the disease, suffer from a significant decrease of efficacy in the
188 later, chronic stage. Moreover, it has been found that some clinical isolates have
189 acquired resistance to the nitro-heterocyclic compounds, and that other strains are
190 innately resistant to these drugs (13). This unsatisfactory situation has led to a
191 sustained effort including clinical trials with posaconazole, E1224, and fexinidazole (14-
192 16), although today, no new drugs for Chagas disease are on the horizon (6).

193 Our aim in this work was the study of previously described anti-kinetoplastid hits
194 bearing an imidazole ring against *T. cruzi*, including an improvement in their
195 pharmaceutical profile through increased polarity. From an initial set of 69 imidazole
196 compounds, 12 derivatives showed promising activities against intracellular *T. cruzi*
197 amastigotes, and acceptable selectivity, and thus deserve future studies (Table S1) (9).
198 However, these imidazoles, all with multiple phenyl substitutions, suffer from sub-
199 optimal solubility. With the aim of decreasing their lipophilicity, we developed a
200 medicinal chemistry strategy that, while retaining the core five-membered ring
201 (imidazole or thiazole) with different substituents, introduces a polar 2-urea bridge to
202 the other part of the molecule, which contains either aromatic or aliphatic tails with
203 different substituents. A series of 26 new imidazoles, closely related to the original hits
204 but with fewer aromatic rings and containing a urea moiety, were synthesized in one-
205 (Scheme 1) or two-step procedures (Scheme 2).

206 The evaluation of the new 26 compounds in a primary *in vitro* screening against
207 a standardized panel of *T. brucei*, *T. cruzi*, *L. Infantum* and mammalian cell lines,
208 showed that five [**23** (NPD-3032), **31** (NPD-3126), **33** (NPD-3024), **37** (NPD-3124) and
209 **38** (NPD-3125)] displayed promising effects against intracellular *T. cruzi* forms (Table
210 1). These findings motivated advanced studies on *T. cruzi* with the most potent

derivatives (IC_{50} < 10 μM). In a first step, the activity in other form of the parasite relevant for human infection, the bloodstream trypomastigotes, was evaluated. For this assay, also another parasite DTU (Y strain belonging to DTU II) was used. From the 17 compounds evaluated (Table 2), five [**2** (NPD-260), **8** (NPD-289), **9** (NPD-274), **31** (NPD-3126) and **33** (NPD-3024)] showed better activity than benznidazole against the bloodstream forms *in vitro*, and we selected **9** (NPD-274) for preliminary cellular studies. Electron microscopy data demonstrated that the major and early ultrastructural insults included flagellar pocket dilatation, disruption of Golgi apparatus, extensive blebs and shedding events of the plasma membrane. These events might be linked to defects in osmoregulation - believed to be one of the functions of cAMP signaling in *T. cruzi* (17). In addition large number of myelin figures were observed, as well as membranous enclosures surrounding cytoplasmic organelles that are the morphological characteristics of autophagy, as reported for other trypanocidal compounds (18). Autophagy is a process involved in life cycle progression and differentiation and in *Leishmania* cAMP signaling has been directly linked to autophagy and differentiation (19). Similarly, cAMP signaling has been implicated in life cycle progression and differentiation in *T. cruzi* (20-22). Thus, our ultrastructural observations are compatible with the phenyl-substituted imidazoles acting through the inhibition of cAMP phosphodiesterases (PDEs), as previously shown in *Leishmania* (9).

Validation measurements of the intracellular and extracellular cAMP content after incubation BT with **9** (NPD-274) were therefore conducted. These experiments were conducted with trypomastigotes as it is impossible to separate out the cAMP of the much bigger host cells from the cAMP inside amastigotes. Lacking an established positive control for the stimulation of cAMP in *T. cruzi*, we utilized two well-characterized inhibitors of *T. brucei* PDE-B1/B2, NPD-001 and NPD-008 (11, 12), relying on the very high level of structural conservation in PDEs between kinetoplastids (23, 24). As expected, both compounds induced a clear and highly significant increase in the cellular cAMP concentration at concentrations of just 2x or 5x their EC_{50} value.

239 Moreover, **9** (NPD-274) similarly induced cAMP increases: 246% of the untreated
240 control at 5x EC_{50} after just 2.5 h of incubation and despite a highly significant increase
241 in cAMP efflux. Interestingly, all three PDE inhibitors also stimulated the efflux of cAMP
242 from the trypomastigotes, significantly raising the cAMP concentration in the medium
243 over that of the control (P <0.001). The phenomenon of cAMP efflux has been
244 described for mammalian cells, where it is mediated by ABC-class transporters (25),
245 but to the best of our knowledge it has not been reported for protozoan cells, although
246 we have previously observed it in *T. brucei* and *Leishmania* species (26). The
247 increased efflux from the trypomastigotes clearly shows that this mechanism in part
248 compensates for the inhibition of phosphodiesterase activities in the cells; however, as
249 the cellular levels still increase significantly, we propose that the efflux mechanism was
250 saturated upon treatment with the PDE inhibitors, leading to toxic cAMP levels and cell
251 death, as previously demonstrated in *T. brucei* (11, 12).
252 Our findings demonstrate a promising *in vitro* activity of a series of phenyl-
253 substituted imidazole derivatives, several being very active against the different
254 parasite forms and strains, especially **9** (NPD-274), which merits further studies in
255 order to contribute to the identification of novel therapies for Chagas disease.
256
257 **MATERIALS AND METHODS**
258 **Compounds studied**. Imidazoles **1**-**12** from Table S1 were prepared following
259 previously described procedures (10) and have a purity ≥95% by HPLC. Detailed
260 synthetic procedures and full characterization of compounds **13**-**38** shown in Scheme 1
261 and 2 are given in the supplemental material.
262 ***In vitro* parasite growth inhibition assays**. An integrated screening was used to
263 define the activity profile of the test compounds from Table 2, using standard assay
264 protocols as previously described (27). A brief description of each model is given. 1/
265 *Leishmania infantum:* amastigotes harvested from the spleen of infected donor
266 hamsters were used for infection. Murine peritoneal macrophages were obtained after

intraperitoneal stimulation with 2% starch in water for 24–48 h and plated in 96-well microplates at 10^4 cells/well. After adding 10^5 amastigotes per well and 5 days of incubation, parasite burdens are microscopically assessed after Giemsa staining*; 2/* *Trypanosoma brucei brucei:* bloodstream forms of a drug sensitive *T. b. brucei* strain are axenically grown in Hirumi-9 medium at 37 ºC under an atmosphere of 5% CO_2. Assays are performed in 96-well tissue culture plates, each well containing 10^4 parasites. After 4 days of incubation, parasite growth is assessed by adding resazurin (Sigma: R7017) and fluorimetric reading after 4 h at 37 ºC; 3/ *Trypanosoma cruzi:* the nifurtimox-sensitive Tulahuen strain (Lac Z transfected) of *T. cruzi* is maintained on MRC-5 cells. Assays are performed in 96-well tissue culture plates, each well containing the compound dilutions together with 3×10^3 MRC-5 cells and 3×10^4 trypomastigotes. After 7 days incubation, colorimetric reading is performed after addition of chlorophenol red β-D-galactopyranoside (CPRG) (Sigma: 10884308001) as substrate; 4/ Cytotoxicity: MRC-5 cells are cultured in MEM medium supplemented with 20 mM L-glutamine, 16.5 mM $NaHCO_3$ and 5% fetal calf serum. Assays are performed at 37ºC and 5% CO_2 in 96-well tissue culture plates with confluent monolayers. After 7 days incubation, cell proliferation and viability are assessed after addition of resazurin and fluorescence reading.

Stock solution of the selected compounds. 20 mM stock solutions of selected compounds from Tables S1 and 1 were prepared in pure dimethyl sulfoxide (DMSO, maximum final concentration of 1% in assays). As a reference drug, *N*-benzyl-2-(2-nitroimidazol-1-yl)acetamide, benznidazole (Bz; Laboratório Farmacêutico do Estado de Pernambuco, Brazil) was used (28).

Mammalian cells. Primary cardiac cells (CC) cultures were obtained from mice embryos and plated onto 0.01% gelatin-coated coverslips in 96-well plates (29). PMM were purified as previously reported (27).

Parasites. Bloodstream trypomastigotes (BT) of Y strain of *T. cruzi* were obtained by cardiac puncture of infected Swiss Webster mice, on the parasitemia peak (29, 30).

295 **Cytotoxicity assays on cardiac cells.** Non-infected CC were incubated at 37 °C for
296 24 h with increasing concentrations of each compound (12.5 up to 200 µM, 1:2 serial
297 dilution) diluted in supplemented DMEM. CC morphology was evaluated by light
298 microscopy and cellular viability of the CC was determined by standardized PrestoBlue
299 test. The results were expressed as the difference in reduction between treated and
300 non-treated cells according to the manufacturer instructions, and the value of LC_{50}
301 (minimum concentration that reduces in 50% the cellular viability) was determined by
302 non-linear regression using a sigmoid curve with a variable slope (31).
303 **Trypanocidal activity.** BT of Y strain ($5x10^6$/mL) were incubated for 24 h at 37 °C in
304 RPMI in the presence or absence of 1:3 serial dilutions of the compounds (0.2 - 50 µM)
305 for determination of parasite death rates through the direct quantification of live
306 parasites by light microscopy. The IC_{50} (compound concentration that reduces the
307 number of live parasites by 50%) was calculated by non-linear regression (32);
308 Selectivity index (SI) is expressed as the ratio between LC_{50} (toxicity for mammalian
309 cells) and the IC_{50} (activity upon the parasite).
310 **Transmission Electron Microscopy.** Bloodstream trypomastigotes from Y strain (5 ×
311 10^6 parasites/mL) were treated with **9** (NPD-274) for 2 h at the concentration
312 corresponding to its 24 h IC_{50} value. The parasites were fixed with 2.5% glutaraldehyde
313 in 0.1 M Na-cacodylate buffer (pH 7.2) at room temperature for 40 min, and postfixed
314 with a solution of 1% OsO_4, 0.8% potassium ferricyanide, and 2.5 mM $CaCl_2$ in the
315 same buffer for 30 min. The samples were washed in PBS, dehydrated in an ascending
316 acetone series, and embedded in epoxy resin. Ultrathin sections (Leica Ultracut; UCT;
317 Leica, Vienna, Austria) were stained with 2% uranyl acetate and lead citrate and
318 examined using an EM10C Zeiss microscope (Oberkochen, Germany) (33).
319 **cAMP measurement.** BT of Y strain ($15x10^6$ parasites/mL) were treated with **9** (NPD-
320 274) compound in the concentration of 2x and 5x the IC_{50} for 2.5 h at 37 °C. After the
321 incubation, the samples were centrifuged at 5000 rpm for 2 min and the supernatant
322 collected. The pellet was resuspended in 100 µL of HCl 0.1 M and incubated at 4 °C for

20 min, followed by centrifugation at 12000 rpm for 10 min and collection of the supernatant. Samples were stored at -80 °C and then analyzed using a cAMP ELISA kit (Cayman Chemicals, Michigan, USA) accordingly to the manufacturer instructions (11). Each experiment was performed independently at least 3 times and all samples were assayed in duplicate.

ACKNOWLEDGEMENTS

Funding from the EC 7th Framework Programme (FP7-HEALTH-2013-INNOVATION-1, PDE4NPD- no. 602666), RICET (RD16/0027/0010), FEDER funds and MECD (Grant FPU15/1465 to V. S.-P.) is acknowledged. MNCS is CNE from FAPERJ and CNPq researcher. Fiocruz, CNPq and FAPERJ are acknowledged.

REFERENCES

1. Lukes J, Butenko A, Hashimi H, Maslov DA, Votypka J, Yurchenko V. 2018. Trypanosomatids are much more than just trypanosomes: Clues from the expanded family tree. Trends Parasitol 34:466-480.
2. Steverding D. 2014. The history of Chagas disease. Parasit Vectors 7:317.
3. http://www.who.int/news-room/fact-sheets/detail/chagas-disease-(american-trypanosomiasis).
4. Schmunis GA, Yadon ZE. 2010. Chagas disease: a Latin American health problem becoming a world health problem. Acta Trop 115:14-21.
5. Chatelain E. 2017. Chagas disease research and development: Is there light at the end of the tunnel? Comput Struct Biotechnol J 15:98-103.
6. Bermudez J, Davies C, Simonazzi A, Real JP, Palma S. 2016. Current drug therapy and pharmaceutical challenges for Chagas disease. Acta Trop 156:1-16.

7. Chatelain E. 2015. Chagas disease drug discovery: toward a new era. J Biomol Screen 20:22-35.
8. Perez-Molina JA, Molina I. 2018. Chagas disease. Lancet 391:82-94.
9. Sebastián-Pérez V, Hendrickx S, Munday JC, Kalejaiye T, Martínez A, Campillo NE, de Koning H, Caljon G, Maes L, Gil C. 2018. Cyclic nucleotide specific phosphodiesterases as potential drug targets for anti-Leishmania therapy. Antimicrob Agents Chemother:e00603-18.
10. Garcia AM, Salado IG, Perez DI, Brea J, Morales-Garcia JA, Gonzalez-Garcia A, Cadavid MI, Loza MI, Luque FJ, Perez-Castillo A, Martinez A, Gil C. 2017. Pharmacological tools based on imidazole scaffold proved the utility of PDE10A inhibitors for Parkinson's disease. Future Med Chem 9:731-748.
11. de Koning HP, Gould MK, Sterk GJ, Tenor H, Kunz S, Luginbuehl E, Seebeck T. 2012. Pharmacological validation of Trypanosoma brucei phosphodiesterases as novel drug targets. J Infect Dis 206:229-237.
12. Blaazer AR, Singh AK, de Heuvel E, Edink E, Orrling KM, Veerman JJN, van den Bergh T, Jansen C, Balasubramaniam E, Mooij WJ, Custers H, Sijm M, Tagoe DNA, Kalejaiye TD, Munday JC, Tenor H, Matheeussen A, Wijtmans M, Siderius M, de Graaf C, Maes L, de Koning HP, Bailey DS, Sterk GJ, de Esch IJP, Brown DG, Leurs R. 2018. Targeting a subpocket in Trypanosoma brucei phosphodiesterase B1 (TbrPDEB1) enables the structure-based discovery of selective inhibitors with trypanocidal activity. J Med Chem 61:3870-3888.
13. Zingales B, Araujo RG, Moreno M, Franco J, Aguiar PH, Nunes SL, Silva MN, Ienne S, Machado CR, Brandao A. 2015. A novel ABCG-like transporter of Trypanosoma cruzi is involved in natural resistance to benznidazole. Mem Inst Oswaldo Cruz 110:433-444.
14. Morillo CA, Waskin H, Sosa-Estani S, Del Carmen Bangher M, Cuneo C, Milesi R, Mallagray M, Apt W, Beloscar J, Gascon J, Molina I, Echeverria LE, Colombo H, Perez-Molina JA, Wyss F, Meeks B, Bonilla LR, Gao P, Wei B,

McCarthy M, Yusuf S, StopChagasInvestigators. 2017. Benznidazole and Posaconazole in Eliminating Parasites in Asymptomatic T. Cruzi Carriers: The STOP-CHAGAS Trial. J Am Coll Cardiol 69:939-947.

15. Torrico F, Gascon J, Ortiz L, Alonso-Vega C, Pinazo MJ, Schijman A, Almeida IC, Alves F, Strub-Wourgaft N, Ribeiro I, Group ES. 2018. Treatment of adult chronic indeterminate Chagas disease with benznidazole and three E1224 dosing regimens: a proof-of-concept, randomised, placebo-controlled trial. Lancet Infect Dis 18:419-430.

16. http://www.dndi.org/diseases-projects/portfolio/fexinidazole-chagas/.

17. Gould MK, de Koning HP. 2011. Cyclic-nucleotide signalling in protozoa. FEMS Microbiol Rev 35:515-541.

18. Santos CC, Lionel JR, Peres RB, Batista MM, da Silva PB, de Oliveira GM, da Silva CF, Batista DGJ, Souza SMO, Andrade CH, Neves BJ, Braga RC, Patrick DA, Bakunova SM, Tidwell RR, Soeiro MNC. 2018. In Vitro, in silico, and in vivo analyses of novel aromatic amidines against Trypanosoma cruzi. Antimicrob Agents Chemother 62:e02205-17.

19. Bhattacharya A, Biswas A, Das PK. 2012. Identification of a protein kinase A regulatory subunit from Leishmania having importance in metacyclogenesis through induction of autophagy. Mol Microbiol 83:548-564.

20. Tagoe DN, Kalejaiye TD, de Koning HP. 2015. The ever unfolding story of cAMP signaling in trypanosomatids: vive la difference! Front Pharmacol 6:185.

21. Gonzales-Perdomo M, Romero P, Goldenberg S. 1988. Cyclic AMP and adenylate cyclase activators stimulate Trypanosoma cruzi differentiation. Exp Parasitol 66:205-212.

22. Fraidenraich D, Pena C, Isola EL, Lammel EM, Coso O, Anel AD, Pongor S, Baralle F, Torres HN, Flawia MM. 1993. Stimulation of Trypanosoma cruzi adenylyl cyclase by an alpha D-globin fragment from Triatoma hindgut: effect

404 on differentiation of epimastigote to trypomastigote forms. Proc Natl Acad Sci U
405 S A 90:10140-10144.
406 23. Jansen C, Wang H, Kooistra AJ, de Graaf C, Orrling KM, Tenor H, Seebeck T,
407 Bailey D, de Esch IJ, Ke H, Leurs R. 2013. Discovery of novel Trypanosoma
408 brucei phosphodiesterase B1 inhibitors by virtual screening against the
409 unliganded TbrPDEB1 crystal structure. J Med Chem 56:2087-2096.
410 24. Shakur Y, de Koning HP, Ke H, Kambayashi J, Seebeck T. 2011. Therapeutic
411 potential of phosphodiesterase inhibitors in parasitic diseases. Handb Exp
412 Pharmacol doi:10.1007/978-3-642-17969-3_20:487-510.
413 25. Godinho RO, Duarte T, Pacini ES. 2015. New perspectives in signaling
414 mediated by receptors coupled to stimulatory G protein: the emerging
415 significance of cAMP efflux and extracellular cAMP-adenosine pathway. Front
416 Pharmacol 6:58.
417 26. Munday JC, Kalejaiye T, de Koning H. unpublished results.
418 27. Cos P, Vlietinck AJ, Berghe DV, Maes L. 2006. Anti-infective potential of natural
419 products: how to develop a stronger in vitro 'proof-of-concept'. J
420 Ethnopharmacol 106:290-302.
421 28. De Araújo JS, Da Silva CF, Batista DG, Da Silva PB, Meuser MB, Aiub CA, da
422 Silva MF, Araújo-Lima CF, Banerjee M, Farahat AA, Stephens CE, Kumar A,
423 Boykin DW, Soeiro MN. 2014. In vitro and in vivo studies of the biological
424 activity of novel arylimidamides against Trypanosoma cruzi. Antimicrob Agents
425 Chemother 58:4191-4195.
426 29. Meirelles MN, de Araújo-Jorge TC, Miranda CF, de Souza W, Barbosa HS.
427 1986. Interaction of Trypanosoma cruzi with heart muscle cells: ultrastructural
428 and cytochemical analysis of endocytic vacuole formation and effect upon
429 myogenesis in vitro. Eur J Cell Biol 41:198-206.
430 30. Batista Dda G, Batista MM, de Oliveira GM, do Amaral PB, Lannes-Vieira J,
431 Britto CC, Junqueira A, Lima MM, Romanha AJ, Sales Junior PA, Stephens CE,

Boykin DW, Soeiro Mde N. 2010. Arylimidamide DB766, a potential chemotherapeutic candidate for Chagas' disease treatment. Antimicrob Agents Chemother 54:2940-2952.

31. Simões-Silva MR, Nefertiti AS, De Araujo JS, Batista MM, Da Silva PB, Bahia MT, Menna-Barreto RS, Pavao BP, Green J, Farahat AA, Kumar A, Boykin DW, Soeiro MN. 2016. Phenotypic screening in vitro of novel aromatic amidines against Trypanosoma cruzi. Antimicrob Agents Chemother 60:4701-4707.

32. Timm BL, da Silva PB, Batista MM, da Silva FH, da Silva CF, Tidwell RR, Patrick DA, Jones SK, Bakunov SA, Bakunova SM, Soeiro Mde N. 2014. In vitro and in vivo biological effects of novel arylimidamide derivatives against Trypanosoma cruzi. Antimicrob Agents Chemother 58:3720-3726.

33. Salomão K, de Souza EM, Carvalho SA, da Silva EF, Fraga CA, Barbosa HS, de Castro SL. 2010. In vitro and in vivo activities of 1,3,4-thiadiazole-2-arylhydrazone derivatives of megazol against Trypanosoma cruzi. Antimicrob Agents Chemother 54:2023-2031.

SCHEME LEGENDS

Scheme 1. Synthesis of substituted *N*-(thiazole-2-yl)urea (**13**-**17**) and *N*-(1*H*-imidazol-2-yl)urea (**18**-**23**) derivatives using isocyanates.

Scheme 2. Synthesis of substituted *N*-(1*H*-imidazol-2-yl)urea derivatives (**24**-**38**) using 1,1'-carbonyldiimidazole (CDI).

FIGURE LEGENDS

Figure 1. Transmission electron microscopy of bloodstream trypomastigotes Y strain untreated (A) and treated with **9** (NPD-274) for 2 h (B-K). The treated parasites exhibited important features that included flagellar pocket dilatation (Frame B; asterisk), disruption of Golgi apparatus (C, F; <>), extensive blebs (E, G, I; arrows) and shedding events (J, K; double arrow) of the plasma membrane, as well as a large number of myelin figures (K; double asterisks) and membranous profiles surrounding cytoplasmic organelles (D, H; arrowhead).

Figure 2. Intracellular (A) and extracellular (B) cAMP levels after incubation of bloodstream trypomastigotes with **9** (NPD-274) and positive controls NPD-001 and NPD-008. All bars represent the average and SEM of three independent experiments, each conducted in duplicate.

469 **Table 1**. *In vitro* antiparasitic activities (IC_{50}-values, μM) of new imidazole derivatives
470 (**13**-**38**).

Compd.	MRC-5	*T. cruzi*	*L. infantum*	*T. brucei*	PMM
13 (NPD-1368)	>64.0	50.5	53.5	>64.0	>64.0
14 (NPD-1369)	>64.0	>64.0	57.4	>64.0	>64.0
15 (NPD-1371)	>64.0	>64.0	49.7	>64.0	>64.0
16 (NPD-1372)	>64.0	>64.0	48.2	>64.0	48.0
17 (NPD-2906)	>64.0	>64.0	36.0	>64.0	36.0
18 (NPD-2903)	19.5	24.5	32.3	32.3	48.0
19 (NPD-2904)	>64.0	>64.0	37.8	>64.0	48.0
20 (NPD-2905)	20.9	26.0	19.9	8.2	48.0
21 (NPD-2907)	12.8	26.5	26.5	>64.0	>64.0
22 (NPD-2908)	>64.0	>64.0	32.5	>64.0	32.0
23 (NPD-3032)	>64.0	7.1	11.7	6.8	>64.0
24 (NPD-3017)	>64.0	>64.0	>64.0	>64.0	>64.0
25 (NPD-3019)	>64.0	>64.0	>64.0	>64.0	>64.0
26 (NPD-3020)	>64.0	>64.0	53.5	>64.0	>64.0
27 (NPD-3021)	>64.0	>64.0	53.5	>64.0	>64.0
28 (NPD-3022)	>64.0	>64.0	19.0	>64.0	32.0
29 (NPD-3023)	>64.0	37.0	15.7	1.8	>64.0
30 (NPD-3121)	>64.0	>64.0	35.1	>64.0	45.2
31 (NPD-3126)	16.9	3.0	30.0	2.1	33.4
32 (NPD-3018)	>64.0	13.5	32.5	>64.0	32.0
33 (NPD-3024)	>64.0	2.2	7.1	6.0	8.0
34 (NPD-3025)	>64.0	54.6	>64.0	>64.0	>64.0
35 (NPD-3026)	>64.0	49.5	>64.0	>64.0	>64.0
36 (NPD-3122)	>64.0	>64.0	49.4	>64.0	54.6
37 (NPD-3124)	>64.0	1.7	29.3	7.1	34.0
38 (NPD-3125)	>64.0	8.1	39.0	19.3	45.2

471 IC_{50} values for inhibition of the growth of *T. cruzi*, *L. infantum*, and *T. brucei* or for cytotoxicity toward
472 human lung fibroblasts (MRC-5 cells) and primary cell cultures of peritoneal mouse macrophages (PMM);
473 Each value is the mean of two independent determinations.
474

475 **Table 2.** Activity (IC_{50} μM) of selected imidazole derivatives against bloodstream
476 trypomastigotes of Y strain, toxicity profile against cardiac cell cultures (LC_{50} μM) and
477 respective selectivity indexes (SI) after 24 h of incubation. Results (IC_{50} values) are
478 presented as Mean ± SD.

Comp.	Bloodstream trypomastigotes Y strain (24 h)	Cardiac cell cultures	SI
1 (NPD-238)	>50	>200	ND
2 (NPD-260)	11.5 ± 0.2	>200	>17
3 (NPD-311)	>50	>200	ND
4 (NPD-306)	29.7 ± 7.3	>200	>7
5 (NPD-299)	27.4 ± 4.7	>200	>7
6 (NPD-301)	16.8 ± 2.7	>200	>12
7 (NPD-305)	>50	>200	ND
8 (NPD-289)	11.1 ± 0.2	>200	>18
9 (NPD-274)	1.2 ± 0.3	>100	>85
10 (NPD-296)	>50	>200	ND
11 (NPD-297)	35.7 ± 2.2	>200	>6
12 (NPD-276)	22.1 ± 0	>100	>4
23 (NPD-3032)	13.9 ± 1.8	65.6	5
31 (NPD-3126)	4.1 ± 1.8	68.6	17
33 (NPD-3024)	4.6 ± 0.1	>200	>44
37 (NPD-3124)	>50	>200	ND
38 (NPD-3125)	15.7 ± 5.8	>200	>13
Benznidazole	12.9 ± 1.9	>1000	>77

479

480

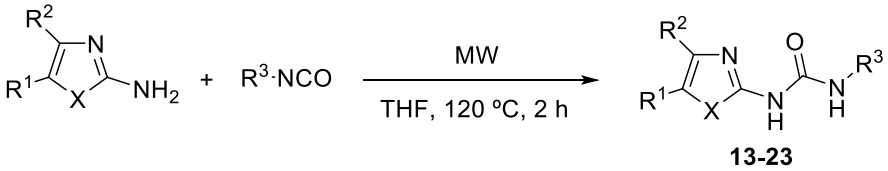

	X	R^1	R^2	R^3
13	S	H	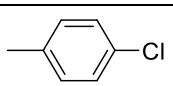	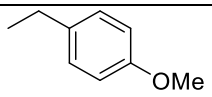
14	S	H	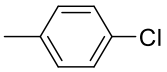	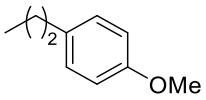
15	S	Me	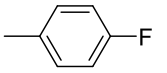	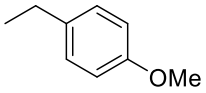
16	S	Me	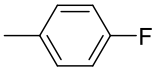	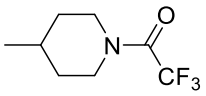
17	S	Me	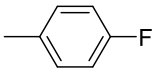	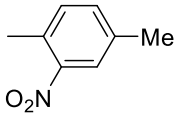
18	NH	H	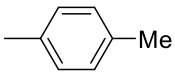	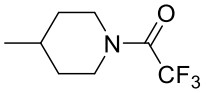
19	NH	H	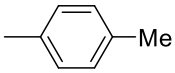	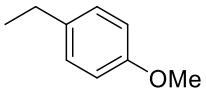
20	NH	H	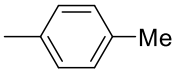	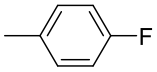
21	NH	H	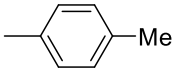	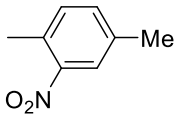
22	NH	H	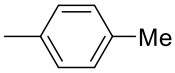	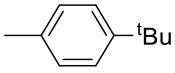
23	NH	H	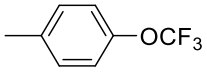	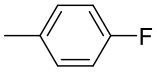

Scheme 1. Synthesis of substituted *N*-(thiazole-2-yl)urea (**13**-**17**) and *N*-(1*H*-imidazol-2-yl)urea (**18**-**23**) derivatives using isocyanates.

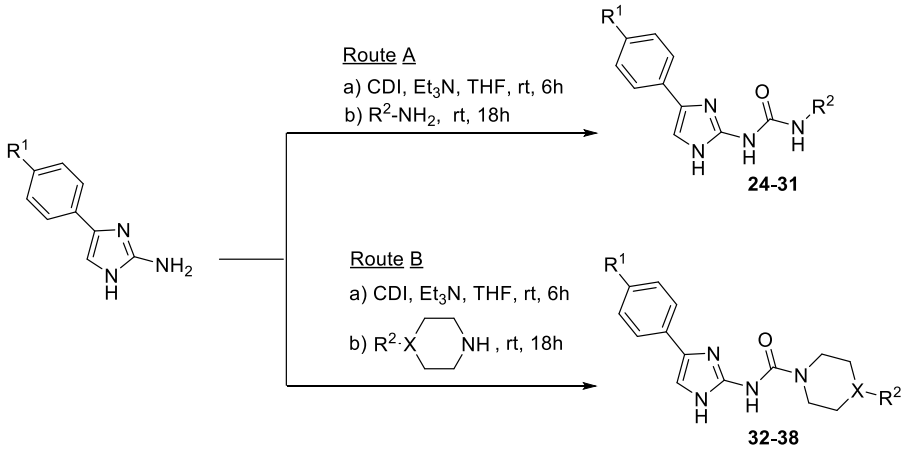

	Route	X	R^1	R^2
24	A	-	Me	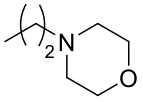
25	A	-	Me	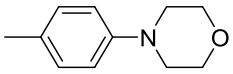
26	A	-	Me	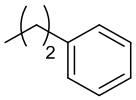
27	A	-	Me	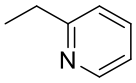
28	A	-	Me	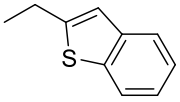
29	A	-	Me	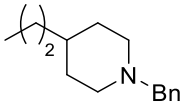
30	A	-	Me	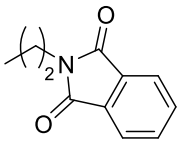

31	A	-		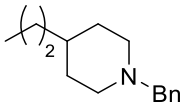
32	B	N	Me	Ph
33	B	C	Me	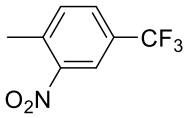
34	B	O	Me	-
35	B	C	Me	CO_2Et
36	B	N	OCF_3	Ph
37	B	C	OCF_3	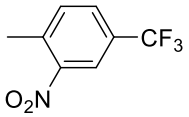
38	B	C		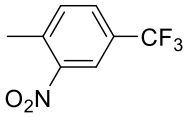

Scheme 2. Synthesis of substituted *N*-(1*H*-imidazol-2-yl)urea derivatives (**24**-**38**) using 1,1'-carbonyldiimidazole (CDI).

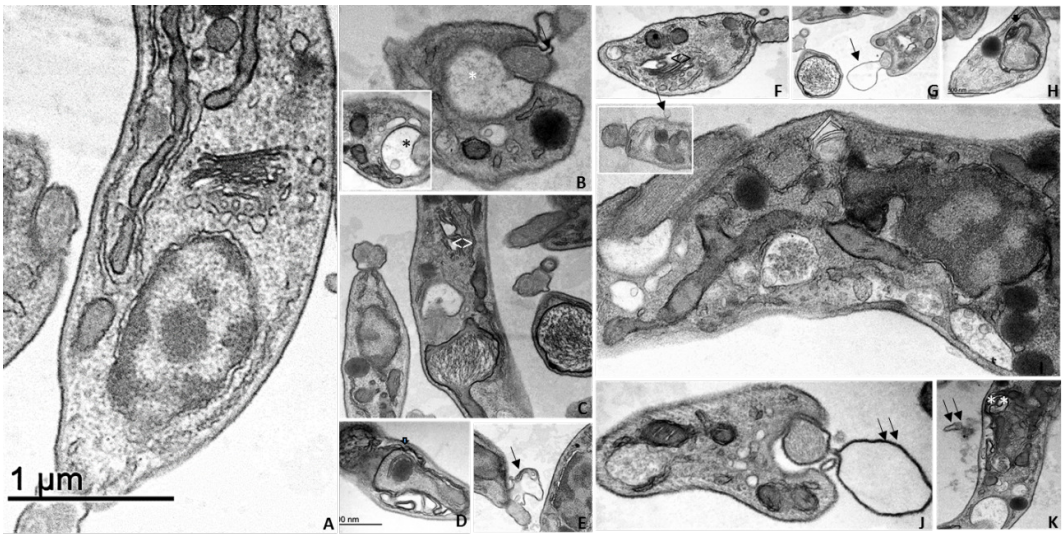

Figure 1. Transmission electron microscopy of bloodstream trypomastigotes Y strain untreated (A) and treated with **9** (NPD-274) for 2 h (B-K). The treated parasites exhibited important features that included flagellar pocket dilatation (Frame B; asterisk), disruption of Golgi apparatus (C, F; <>), extensive blebs (E, G, I; arrows) and shedding events (J, K; double arrow) of the plasma membrane, as well as a large number of myelin figures (K; double asterisks) and membranous profiles surrounding cytoplasmic organelles (D, H; arrowhead).

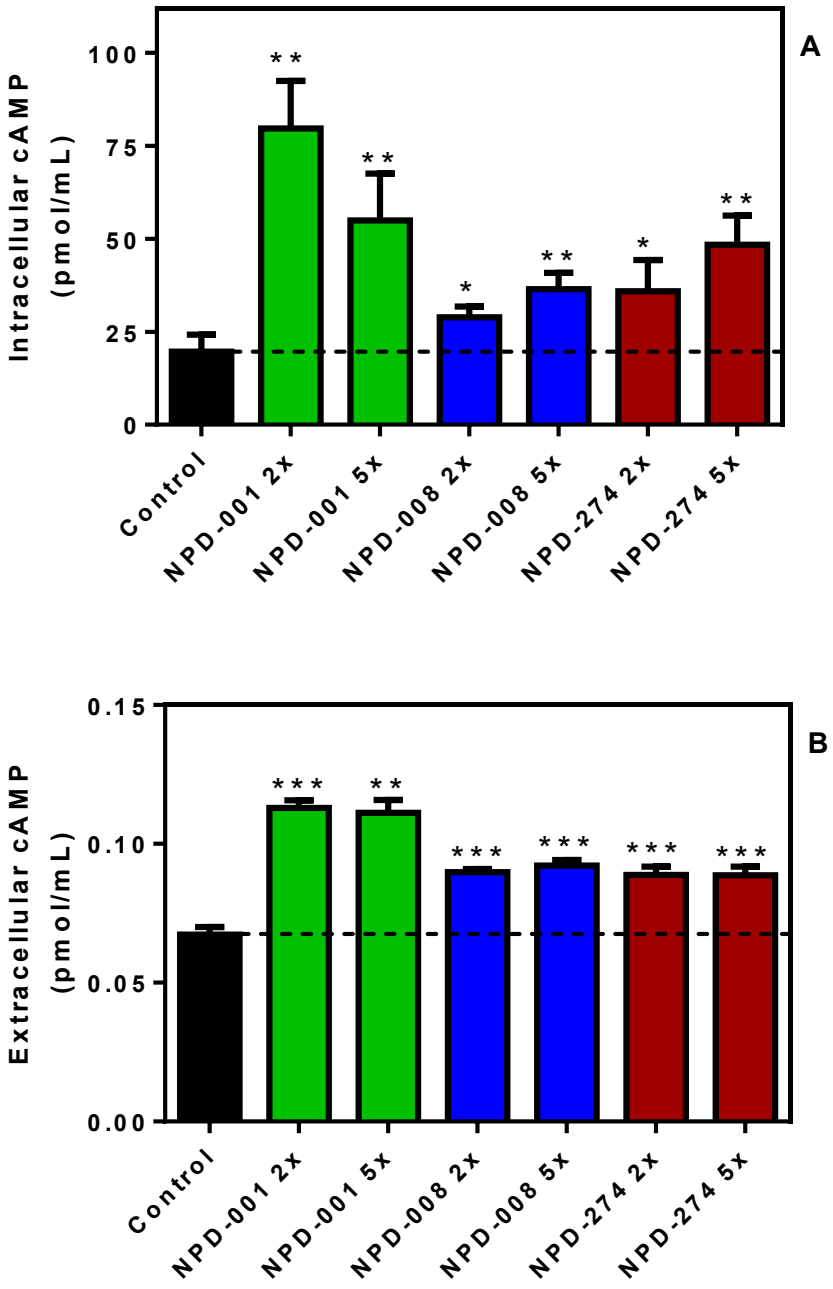

Figure 2. Intracellular (A) and extracellular (B) cAMP levels after incubation of bloodstream trypomastigotes with **9** (NPD-274) and positive controls NPD-001 and NPD-008. All bars represent the average and SEM of three independent experiments, each conducted in duplicate.